arXiv:cond-mat/0108195v2 [cond-mat.soft] 14 Aug 2001

Formation and Decay of Vortex Lattices in Bose-Einstein Condensates at Finite Temperatures

J.R. Abo-Shaeer*, C. Raman†, and W. Ketterle
Department of Physics, MIT-Harvard Center for Ultracold Atoms, and Research Laboratory of Electronics,
MIT, Cambridge, MA 02139

(February 1, 2008)

The dynamics of vortex lattices in stirred Bose-Einstein condensates have been studied at finite temperatures. The decay of the vortex lattice was observed non-destructively by monitoring the centrifugal distortions of the rotating condensate. The formation of the vortex lattice could be deduced from the increasing contrast of the vortex cores observed in ballistic expansion. In contrast to the decay, the formation of the vortex lattice is insensitive to temperature change.

PACS 03.75.Fi, 67.40.Vs, 32.80.Pj

Gaseous Bose-Einstein condensates (BEC) have become a testbed for many-body theory. The properties of a condensate at zero temperature are accurately described by a nonlinear Schrödinger equation. More recently, theoretical work on the ground state properties of condensates [1] has been extended to rotating condensates containing one or several vortices [2] and their dynamics. These include vortex nucleation [3,4], crystallization of the vortex lattice [5], and decay [6,7]. Experimental study has focused mainly on the nucleation of vortices, either by stirring condensates directly with a rotating anisotropy [8–10] or creating condensates out of a rotating thermal cloud [11]. Here we report the first quantitative investigation of vortex dynamics at finite temperature. The crystallization and decay of a vortex lattice have been studied and a striking difference is found between the two processes: while the crystallization is essentially temperature independent, the decay rate increases dramatically with temperature.

The method used to generate vortices has been outlined in previous work [9,12]. Condensates of up to 75 million sodium atoms ($>$ 80% condensate fraction) were prepared in a cigar-shaped Ioffe-Pritchard magnetic trap using evaporative cooling. The radial and axial trap frequencies of $\omega_x = 2\pi \times (88.8 \pm 1.4)$ Hz, $\omega_y = 2\pi \times (83.3 \pm 0.8)$ Hz, and $\omega_z = 2\pi \times (21.1 \pm 0.5)$ Hz, respectively, corresponded to a radial trap asymmetry of $\epsilon_r = (\omega_x^2 - \omega_y^2)/(\omega_x^2 + \omega_y^2) = (6.4 \pm 0.2)\%$ and an aspect ratio of $A = \omega_x/\omega_z = (4.20 \pm 0.04)$. The relatively large value of the radial trap asymmetry is due to gravitational sag and the use of highly elongated pinch coils (both estimated to contribute equally). The radio frequency used for evaporation was held at its final value to keep the temperature of the condensate roughly constant throughout the experiment. The condensate's Thomas-Fermi radii, chemical potential, and peak density were $R_r = 28$ μm, $R_z = 115$ μm, 300 nK, and 4×10^{14} cm^{-3}, respectively, corresponding to a healing length $\xi \simeq 0.2$ μm.

Vortices were produced by spinning the condensate for 200 ms along its long axis with a scanning, blue-detuned laser beam (532 nm) [8,13]. For this experiment two symmetric stirring beams were used (Gaussian waist $w = 5.3$ μm, stirring radius 24 μm). The laser power of 0.16 mW per beam corresponded to an optical dipole potential of 310 nK. After the stirring beams were switched off, the rotating condensate was left to equilibrate in the static magnetic trap for various hold times. As in our previous work, the vortex cores were observed using optical pumping to the $F = 2$ state and resonant absorption imaging on the $F = 2$ to $F = 3$ cycling transition [9]. After 42.5 ms of ballistic expansion the cores were magnified to 20 times their size, ξ, in the trap.

The decay of the vortex lattice can be observed by allowing the condensate to spin down in the trap for variable times before the ballistic expansion and subsequent observation of the vortex cores. However, this method requires destructive imaging and suffers from shot-to-shot variations. *In situ* phase-contrast imaging is non-destructive, but the vortex cores are too small to be resolved. Instead, we monitored the centrifugal distortion of the cloud due to the presence of vorticity. This is a quantitative measure for the rotation frequency, Ω, of the lattice, and therefore the number of vortices [14]. Such distorted shapes have been observed previously for rotating clouds [9,11,12].

The shape of a rotating condensate is determined by the magnetic trapping potential and the centrifugal potential $-\frac{1}{2}M\Omega^2 r^2$, where M is the atomic mass. From the effective radial trapping frequency $\omega_r \rightarrow \omega_r' = \sqrt{\omega_r^2 - \Omega^2}$, one obtains the aspect ratio of the rotating cloud, $A' = \omega_r'/\omega_z$, as

$$A' = A\sqrt{1 - (\Omega/\omega_r)^2}. \tag{1}$$

For the decay measurements, the condensate was stirred for 200 ms, producing $\sim$ 130 vortices on average at the coldest temperature (determined using time-of-flight imaging). After the drive was stopped the cloud equilibrated in the stationary magnetic trap. Ten *in situ* images of each condensate were taken at equal time intervals using non-destructive phase contrast imaging detuned 1.7 GHz from resonance (see Fig. 1a). We verified that the decay was not affected due repeated imaging by varying the time between exposures and observing no difference. The theoretical treatment of the decay has two limiting cases, one where the thermal cloud is nearly stationary, the other where the thermal cloud is closely following the rotating condensate [6]. Because the thermal cloud could not easily be discerned in images taken with 1.7 GHz detuning, we used light closer to resonance (400 MHz detuning) to determine the shape of the thermal cloud (Fig. 1b).

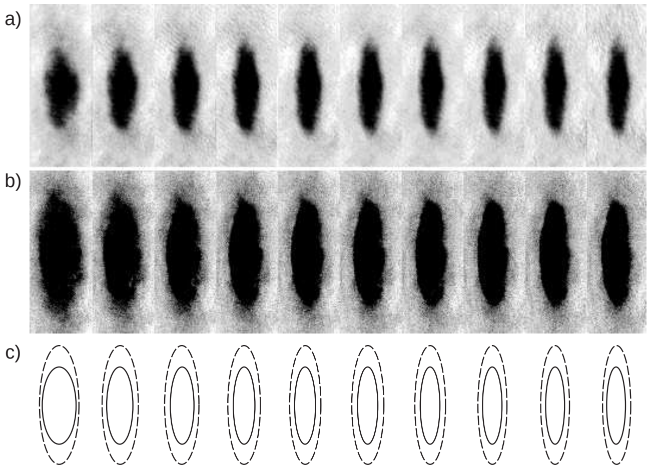

FIG. 1. a) Spin down of a rotating condensate in a static magnetic trap. The first phase contrast image is taken 100 ms after turning off the drive, with each subsequent image spaced by 100 ms. The rotating vortex lattice caused a radial swelling of the condensate, reducing the aspect ratio. As vortices leave the system the aspect ratio approaches its static value of 4.20. The field of view is 25 μm by 75 μm. b) Observation of a rotating thermal cloud. The parameters are identical to (a), but the probe light detuning is closer to resonance, enhancing the sensitivity to the more dilute thermal cloud. The phase shift of the dense condensate exceeds 2π and is displayed as saturated in the image. The apparent loss in atom number is due to Rayleigh scattering of the probe light. c) The inner and outer contours represent the aspect ratio of the condensate and thermal cloud, respectively, as obtained from two-dimensional fits to phase-contrast images.

The aspect ratio of the condensate was obtained by fitting a 2D Thomas-Fermi profile to the 1.7 GHz images. The aspect ratio of the thermal cloud was determined from the 400 MHz images by masking off the condensate in the inner region of the cloud, and then fitting a 2D Gaussian to the image. The comparison of the contours of the condensate and thermal cloud (condensate fraction of $N_c/N = 0.62$) shows that the thermal cloud is also rotating. The images for the thermal cloud show that the aspect ratio decays from 3.0 to 4.2 on the same time scale as the condensate. This corresponds to an initial rotation rate of $\sim 2/3$ that of the condensate.

The damping rate of the vortex lattice, obtained from exponential fits to the data, was studied at different temperatures by varying the condensed fraction of atoms in the trap. The condensate fractions were obtained from fits to time-of-flight images of the condensate *before* the stirring. The temperature was derived from these values using the scaling theory for an interacting Bose gas [15]. At a fixed rf frequency for evaporation, the centrifugal potential lowers the trap depth by a factor $1 - (\Omega/\omega_r)^2$ for a thermal cloud rotating at frequency Ω. Evaporation should lower the temperature of the rotating cloud by the same factor.

Fig. 2a shows how the aspect ratio of the condensate approaches its static value as the vortex lattice decays. The decrease of the angular speed appears to be exponential (Fig. 2b) and strongly depends on temperature (Fig. 3).

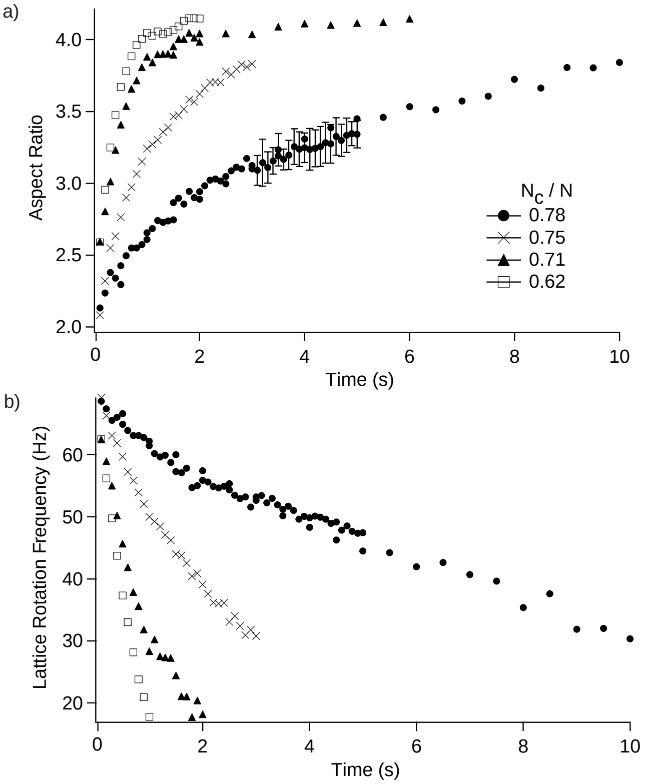

FIG. 2. Decay of a vortex lattice at finite temperatures. a) The aspect ratio of the condensate approaching its static value. Each point represents the average of 10 measurements. Error bars given for (●) are statistical and are typical of all four data sets. b) The decay of the rotation rate of the lattice for the same data using Eq. (1). The decay of the rotation depends strongly on the thermal component.

In addition to the decay process, the formation of the vortex lattice has also been examined. After rotating the condensate it typically took hundreds of ms for the lattice to form (see Fig. 4 in ref. [9]). One may expect the lattice to already form in the rotating frame during the stirring because the lattice is the lowest energy state for a given angular momentum. This absence of equilibration in the rotating frame is presumably due to heating and excitation of collective lattice modes by the stirring beams. The crystallization of the vortex lattice was studied by determining the contrast or visibility of the vortex cores as a function of equilibration time. To avoid any bias, we used an automated vortex recognition algorithm. First, each image was normalized by dividing it by a blurred duplicate of itself. A binary image was then created with a threshold set to the value at which the algorithm reliably detected almost all vortices that were identified by visual inspection of equilibrated images (there was less than 5% discrepancy). Clusters of contiguous bright pixels within a circular area were counted as "visible" vortices. Fig. 4a shows three vortex lattices after different equilibration times with the visible vortices identified.

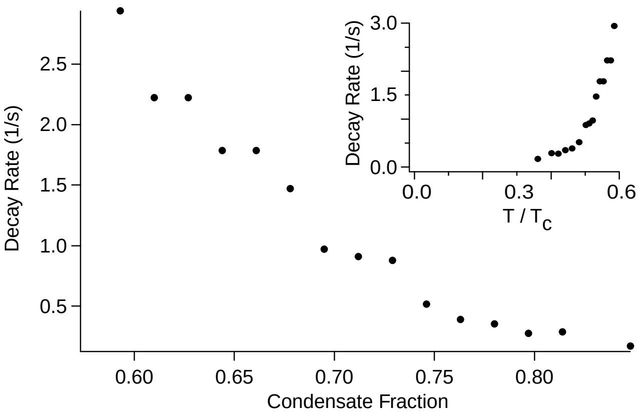

FIG. 3. Decay rates for vortex lattices at several temperatures. The rates are determined from data taken during the 1st second of equilibration. Each point represents the average of 5 measurements. The inset figure emphasizes the strong dependence of the decay rate on temperature, T. The transition temperature was $T_c = 790$ nK and varied by less than 7 % for the data shown.

The lowest temperature (337 nK, corresponding to a condensate fraction of $\approx 80\%$) was close to the chemical potential. Further cooling would have resulted in smaller condensates. The highest temperature (442 nK) was limited by the rapid decay of the vortex lattice.

Fig. 4b,c show that the formation of the lattice depends very weakly on temperature, if at all, over the range studied. The larger number of vortices crystallized at lower temperatures (Fig. 4b) is due to the strong temperature dependence of the lattice decay rates, which differed by more than a factor of 5. We can correct for this by estimating the number of vortices $N_v(t)$ as a function of time from the centrifugal distortion measurements described above as $N_v(t) = 2\kappa\Omega(t)\pi R(t)^2$, where $\kappa = h/M$ is the quantum of circulation, M the sodium mass and R the radial Thomas-Fermi radius. By normalizing the number of visible vortices by this estimate, we deduce the vortex visibility as a function of time. These lattice formation curves overlap almost perfectly for different temperatures (Fig. 4c).

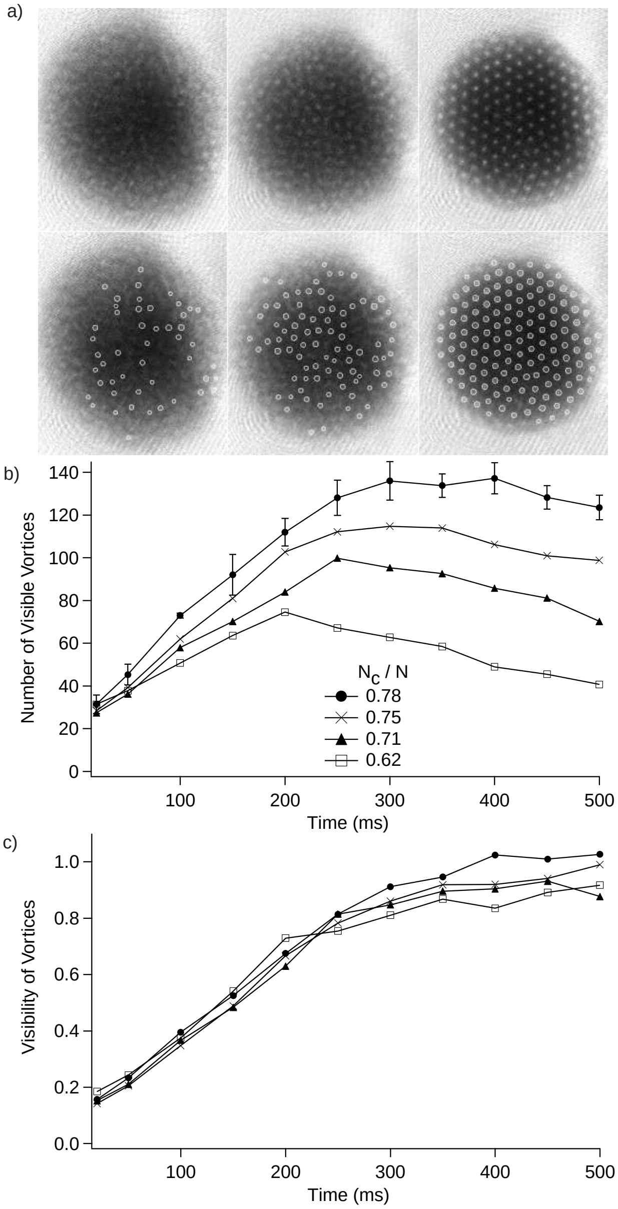

FIG. 4. Crystallization of the vortex lattice. a) The top row shows three condensates that have equilibrated for 50, 150 and 300 ms, respectively, and have 48, 86 and 140 vortices recognized as "visible" by our algorithm. The bottom row shows the same condensates with the "visible" vortices circled. The field of view was 1.4 mm by 1.6 mm. b) Growth of the number of visible vortices for several temperatures expressed by the condensate fraction (N_c/N). c) Visibility of vortices derived from the data in figure b, normalized by the number of vortices inferred from centrifugal distortion measurements.

The decay of a vortex lattice is discussed in refs. [6,7]. The process is modelled as a two-step transfer of angular momentum. The rotation of the condensate is damped due to friction with the thermal cloud (μ_{c-th}), which is in turn damped via friction with the trap anisotropy ($\mu_{th-\epsilon_r}$). Even at our highest temperatures, μ_{c-th} is sufficiently larger than $\mu_{th-\epsilon_r}$ to spin up the thermal cloud to $\sim 2/3$ of the lattice rotation rate. $\mu_{th-\epsilon_r}$ is calculated in ref. [16] for a classical Boltzmann gas. For our parameters the relaxation time $\tau_{\rm rot}$ for the thermal cloud rotation is $\tau_{\rm rot} = 4\tau$, where τ is the relaxation time for quadrupolar deformations. τ is approximately 5/4 of the time between elastic collisions $\tau_{\rm el} = 2/n v_{\rm th}\sigma$ [17], where n is the atomic density, $v_{\rm th}$ the thermal velocity and σ the elastic cross section. For a quantum-saturated thermal cloud, this gives a relaxation time proportional to T^{-2}.

The presence of the condensate adds additional moment of inertia, extending the rotational relaxation time by a factor $f_{\rm inertia} = (I_{\rm th} + I_c)/I_{\rm th}$, where $I_{\rm th}$ and I_c are the moments of inertia of the thermal cloud and the condensate, respectively. At high temperatures this factor approaches one, because the moment of inertia of the thermal cloud is dominant. For very low temperatures $f_{\rm inertia} \sim (I_c \ / \ I_{th})$. This ratio is [6]

$$\frac{I_c}{I_{\rm th}} = \frac{15\zeta(3)}{16\zeta(4)} \frac{N_c}{N_{\rm th}} \frac{\mu}{k_B T} \tag{2}$$

where the numerical pre-factor is 1.04. Thus, for a non-interacting Bose gas in the low temperature limit $f_{\rm inertia}$ scales as T^{-4} and the relaxation time of the vortex lattice should scale as T^{-6}. The observed temperature dependence of the relaxation time, decreasing by a factor of 17 for a 60% increase in the temperature, agrees fortuitously well given the approximations made in the theory. The absolute relaxation rates predicted by refs. [6,16] are on the order of 1 s^{-1}, in reasonable agreement with our results. However, for a quantitative comparison to theory it will be necessary to further characterize the rotating thermal cloud, which may not be in full equilibrium.

In contrast to the decay, the crystallization process of the vortex lattice was essentially independent of temperature. This was unexpected because all dissipative processes observed thus far in BECs, including the decay of the vortex lattice, have shown a strong temperature dependence [18,19]. D. Feder has numerically simulated a stirred condensate using only the Gross-Pitaevskii equation. The results show that the absence of dissipation leads to rapid, irregular motion of the vortices. The addition of a phenomenological dissipative term in ref. [5] resulted in the formation of triangular vortex lattices. However, the origin of the dissipation was not identified. Our results suggest that the time-limiting step for the evolution of a vortex tangle into a regular lattice does not strongly depend on temperature. One possibility is that the thermal cloud is not directly involved. This may be similar to the reconnection of vortices or the damping of Kelvin modes, where the spontaneous emission of phonons act as a dissipative mechanism [20,21]. Another possibility is that the rearrangement of the vortices into a rectilinear lattice is slow and not limited by dissipation.

In conclusion, we have studied the crystallization and decay of vortex lattices. Both processes are dissipative and require physics beyond the Gross-Pitaevskii equation. The dynamics of vortices nicely illustrates the interplay of experiment and theory in the field of BEC.

The authors would like to acknowledge T. Rosenband for development of the vortex recognition algorithm. We also thank J.M. Vogels and K. Xu for their experimental assistance and J.R. Anglin, Z. Hadzibabic, A.E. Leanhardt, and R. Onofrio for insightful discussions. This research is supported by NSF, ONR, ARO, NASA, and the David and Lucile Packard Foundation.

---

[*] Contact Information: jamil@mit.edu

[†] Present address: School of Physics, Georgia Institute of Technology Atlanta, Georgia 30332-0430 USA

[1] F. Dalfovo, S. Giorgini, L. P. Pitaevskii, and S. Stringari, Rev. Mod. Phys. **71**, 463 (1999).

[2] A. L. Fetter and A. A. Svidzinsky, J. Phys.: Condens. Matter **13**, R135 (2001).

[3] F. Dalfovo and S. Stringari, Phys. Rev. A **63**, 011601 (2001).

[4] J. R. Anglin, preprint cond-mat/0106619.

[5] M. Tsubota, K. Kasamatsu, and M. Ueda, preprint cond-mat/0104523.

[6] O. N. Zhuravlev, A. E. Muryshev, and P. O. Fedichev, preprint cond-mat/0007246.

[7] P. O. Fedichev and A. E. Muryshev, preprint, cond-mat/0004264.

[8] K. W. Madison, F. Chevy, W. Wohlleben, and J. Dalibard, Phys. Rev. Lett. **84**, 806 (2000).

[9] J. R. Abo-Shaeer, C. Raman, J. M. Vogels, and W. Ketterle, Science **292**, 476 (2001).

[10] E. Hodby, G. Hechenblaikner, S. A. Hopkins, O. M. Maragò, and C.J.Foot, preprint cond-mat/0106262.

[11] P. C. Haljan, I. Coddington, P. Engels, and E. A. Cornell, preprint cond-mat/0106362.

[12] C. Raman, J. R. Abo-Shaeer, J. M. Vogels, K. Xu, and W. Ketterle, preprint cond-mat/0106235.

[13] R. Onofrio, D. S. Durfee, C. Raman, M. Köhl, C. E. Kuklewicz, and W. Ketterle, Phys. Rev. Lett. **84**, 810 (2000).

[14] P. Nozières and D. Pines, *The Theory of Quantum Liquids* (Addison-Wesley, Redwood City, CA, 1990).

[15] S. Giorgini, L. P. Pitaevskii, and S. Stringari, J. Low Temp. Phys. **109**, 309 (1997).

[16] D. Guéry-Odelin, Phys. Rev. A **62**, 033607 (2000).

[17] D. Guéry-Odelin, F. Zambelli, J. Dalibard, and S. Stringari, Phys. Rev. A **60**, 4851 (1999).

[18] D. S. Jin, M. R. Matthews, J. R. Ensher, C. E. Wieman, and E. A. Cornell, Phys. Rev. Lett. **78**, 764 (1997).

[19] D. M. Stamper-Kurn, H.-J. Miesner, S. Inouye, M. R. Andrews, and W. Ketterle, Phys. Rev. Lett. **81**, 500 (1998).

[20] M. Leadbeater, T. Winiecki, D. C. Samuels, C. F. Barenghi, and C. S. Adams, Phys. Rev. Lett. **86**, 1410 (2001).

[21] D. Kivotides, J.C. Vassilicos, D.C. Samuels, and C.F. Barenghi, Phys. Rev. Lett. **86**, 3080 (2001).